



## FRAGILITY CURVES FOR SEISMIC VULNERABILITY ASSESSMENT OF REINFORCED CONCRETE FRAME BUILDINGS IN CANADA

A. Al Mamun<sup>(1)</sup>, M. Saatcioglu<sup>(2)</sup>

<sup>(1)</sup> PhD Candidate, Department of Civil Engineering, University of Ottawa, amamu022@uottawa.ca

<sup>(2)</sup> Distinguished University Professor and University Research Chair, Department of Civil Engineering, University of Ottawa, Murat.Saatcioglu@uottawa.ca

### Abstract

Performance of reinforced concrete frame buildings in recent earthquakes indicates variations in damage levels depending on the seismic hazard of the region and the vulnerability of structures. While older buildings that lack proper seismic design and detailing practices suffer the most damage, newer buildings perform better, but are still expected to suffer different degrees of damage depending on the level of ground excitation and the stringency of design employed. Performance-based evaluation of buildings requires fragility curves for different levels of performance. Commonly accepted performance limits include; immediate occupancy, life safety and collapse prevention. The objective of this paper is to present seismic fragility curves generated for different limit states, where the intensity of hazard is expressed in terms of spectral accelerations, and the building performance is expressed in terms of maximum inter-storey drift.

Two reinforced concrete frame buildings with 5-stories were considered for the development of fragility curves, for a building period typically encountered in practice. The buildings were designed to represent post-1985 era construction in Canada. They represented a moderately ductile building in Ottawa subjected to eastern Canadian seismicity and a fully ductile building in Vancouver subjected to western Canadian seismicity. The buildings were analyzed using PERFORM-3D software to assess their seismic vulnerabilities. Incremental Dynamic Analysis (IDA) was employed with different scale factors to generate the fragility curves. Two sets of earthquake records compatible with uniform hazard spectra (UHS) of 2010 NBCC were selected, where each set contained 20 records for each city. The fragility curves depict probabilities of exceedances for different damage states, and can be used for seismic vulnerability assessment of 5-storey reinforced concrete frame buildings in Canada, representing mid-rise construction designed and built after 1985.

*Keywords: RC Frame, PERFORM-3D, Fragility curve, Ductile, Moderately Ductile*

### 1. Introduction

Frequent earthquakes occur in Canada with significant historical damage. The seismic hazard in Canada can be characterized by the seismicity of two distinct regions; eastern Canada and western Canada with a relatively stable central region between the two. Significant seismic activities occur in western Canada because of the presences of active faults along the Pacific Rim. Geological Survey of Canada records more than 1000 earthquakes annually in western Canada with more than 100 earthquakes of magnitude 5 or greater. Seismic activity in eastern Canada occurs with reduced frequency of approximately 500 earthquakes annually, with approximately 3-magnitude 5 earthquakes taking place in each decade [1]. Eastern Canada does not have active faults. The earthquakes in this region are believed to be related to the regional stress fields with earthquakes concentrated in regions of crustal weakness. Stronger earthquakes are expected in the west, though damaging earthquakes have also occurred in the east. Eastern earthquakes tend to be less frequent and of moderate magnitude. This difference in seismic regions is reflected in building design practices that follow the requirements of the National Building Code of Canada (NBCC).

It is preferable to conduct seismic vulnerability assessment of buildings through dynamic inelastic response history analyses. However, this may not be feasible for the majority of buildings. An alternative is to conduct fragility analysis using fragility curves that incorporate design characteristics of the building being assessed. The objective of this paper is to present seismic fragility curves for mid-rise reinforced concrete frame buildings in

Canada, designed and built after 1985. It forms part of a comprehensive research program currently underway at the University of Ottawa involving reinforced concrete frame and shear wall buildings, and unreinforced masonry buildings, with or without irregularities, designed during different periods of building code development.

The building inventory in Canada can be viewed in two broad groups; those designed prior to the enactment of modern seismic codes, and those designed using the more recent seismic hazard values and building design and detailing practices. The design base shear equation in NBCC has changed since the inception of seismic provisions in 1941 [2]. Earlier equations defined seismic base shear as a percentage of seismic weight of buildings in the form of a seismic coefficient. In the 1953 NBCC [3], the building height was introduced as a design parameter, crudely reflecting the effect of building period on seismic coefficient. In the 1965 NBCC [4], the difference in construction type and associated level of ductility was introduced through coefficient  $C$ , reducing base shear for reinforced concrete frame and shear wall buildings with ductile detailing while increasing it for non-ductile buildings. In the 1970 NBCC [5] the effect of construction type, reflecting the associated level of ductility, was treated more extensively through coefficient  $K$ . Empirical expressions were also introduced for the computation of fundamental period. This was followed by the 1975 NBCC [6] Commentary with ductility factors for different building types for use in dynamic analysis. The requirements remained essentially the same in the 1980 NBCC [7] with refinements made to seismic response coefficient  $S$  as affected by fundamental period. The hazard values were introduced through seismic maps with seismic zones for different regions, which were introduced in 1953 and revised in 1970. New seismic zoning maps were introduced in the 1985 NBCC [8] with seismic velocity and acceleration ratios specified for each zone, refining hazard values significantly based on 10% probability of exceedance in 50 years. Further refinements were introduced to the seismic response coefficient  $S$  with a new empirical period equation provided for shear wall buildings. The ductility related construction type factor  $K$  was replaced by force modification factor  $R$  in 1990 [9], with a calibration factor  $U$ , which introduced a reduction in base shear to account for structural over-strength and to bring the force levels to levels consistent with the safety implied in earlier codes. The same base shear expression remained essentially the same until 2005 [10], with a revised empirical equation introduced for fundamental period of shear wall buildings. Significant changes were introduced in 2005 with new site specific uniform hazard spectra having 2% in 50-year probability of exceedance. The approach was kept the same in the 2010 NBCC [11] with new hazard values introduced in the 2015 NBCC [12].

The design and detailing requirements for reinforcement concrete buildings in CSA A23.3 (CSA) went through a similar evolution. There were no seismic design requirements prior to CSA A23.3-1973 [13], which was referenced in the 1975 NBCC. Ductile design and detailing requirements for seismic resistance were introduced for the first time in 1973, which remained the same until 1984. Significant improvements were made to the standard in 1984 with the introduction of capacity design requirements, protecting critical elements and preventing non-ductile failures. Three levels of seismic detailing were specified for the first time for: i) ductile response, ii) moderately ductile response, and iii) frame members that are not part of the seismic resisting system but “go for the ride” during seismic response. Critical elements in ductile buildings were protected and non-ductile failure modes were prevented by increasing design levels to those associated with the development of probable moment resistances in plastic hinges at 125% of the steel yield strength. The same capacity design concept was implemented in nominally ductile buildings using nominal capacities. The stringency of design depended on the design ductility demand selected in the 1985 NBCC, which made reference to CSA A23.3-1984 [14]. Hence, 1985 was taken as the “benchmark” year for significant improvements in seismic design of reinforced concrete buildings in Canada. The same year had also been adopted as the bench mark year in the Canadian seismic screening manual [15].

An extensive comparison of seismic demands and capacities of reinforced concrete frame buildings was performed as part of the current investigation to assess the significance of variations in building designs between 1985 and 2015. Static seismic base shears for the 5-storey buildings used in the current investigation were calculated. Fig. 1 shows the evolution of seismic design base shear ratio (design base shear,  $V$ /building weight used for base shear calculations,  $W$ ). It was observed that the change in equivalent seismic base shear (based on the empirical code period) was 1.2 times the 1985 value for the moderately ductile building in Ottawa and 1.4 times the 1985 value for the ductile building in Vancouver. However, this change did not translate into

equivalent changes in final building designs. The seismic load combinations changed from  $1.25D+0.7(1.5L+1.5E)$  in 1985 to  $1D+0.5L+1E$  starting in 1990, implying that the contribution of gravity loads to member design would be higher in 1985 when seismic forces were lower, whereas the effects of gravity loads would be relatively lower in the post 1990 codes when the base shear was higher. The changes in load factors offset the final designs to a certain degree. Furthermore, the concrete resistance factor,  $\phi_c$  was 0.6 in CSA A23.3-1984, whereas it was increased to 0.65 in CSA A23.3-2004 [16], resulting in reduced nominal capacities of members in post 2005 NBCC designs. Therefore, the final structural designs of the buildings considered did not show significant variations in member designs. Hence, reinforced concrete frame buildings designed between 1985 and 2015 were grouped together for the purpose of seismic vulnerability assessment.

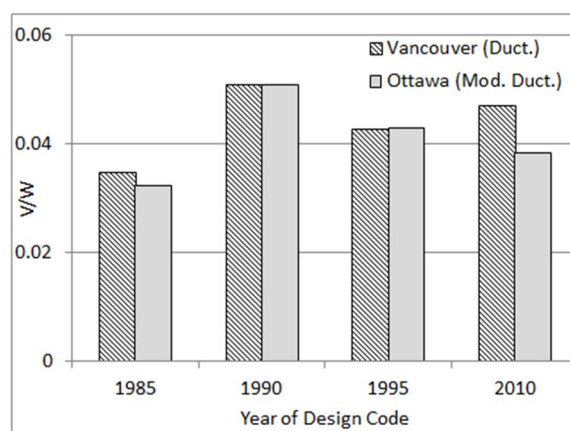


Fig. 1 – Base shear evolution of 5-storey building located in Ottawa and Vancouver according to NBCC

## 2. Selection and Design of Buildings

Two regular frame buildings with a 5-storey height were selected, one for Ottawa and the other for Vancouver. The buildings consisted of moment resisting frames in both orthogonal directions with 5 bays in each direction, with a 7.0 m span length, resulting in a 35m by 35m square floor plan. A typical floor height of 4.0 m was used for each floor, including the ground level. The design dead load included a superimposed dead load of 1.33 kPa in addition to member self-weight. The live load was 2.4 kPa.

The buildings were designed based on the 2010 NBCC seismic requirements with the accompanying CSA Standard A23.3-04 “Design of Concrete Structures” used for proportioning and detailing of members. The equivalent static load approach was used to compute elastic seismic base shear ( $V_e$ ). The buildings were designed for residential occupancy with an importance factor of  $I = 1.0$  on firm soil (Soil Class C). The fundamental period was computed by performing Eigen Value analysis through the use of SAP 2000 software based on reduced section properties according to CSA A23.3-04. These dynamic fundamental periods were longer than those computed by the code-recommended empirical values. Therefore, the period values were taken as 1.5 times the values computed based on the empirical code equations for design. Uniform Hazard Spectra (UHS) values were used for design as prescribed in the 2010 NBCC. These corresponded to spectral accelerations ( $S_a$ ) of 0.134g for the building in Ottawa and 0.320g for the building in Vancouver. The building in Ottawa consisted of moderately ductile frames designed with ductility related force modification factor  $R_d$  and over-strength related force modification factor  $R_o$  as 2.5 and 1.4, respectively. The building in Vancouver consisted of fully ductile frames, designed with  $R_d = 4.0$  and  $R_o = 1.7$ . Concrete compressive strength,  $f'_c$ , was taken as 30 MPa. Reinforcing steel with 400 MPa yield strength was used in all members. The buildings were analyzed and designed by using software ETABS [17] with the load cases defined in 2010 NBCC. Table 1 shows the design details for each member. Since design base shears of moderately ductile and ductile structures were close, as shown in Fig.1, both eastern and western structures had the same member properties. Yield moments were also similar, with slightly different ultimate moment capacities because of the differences in the ductility ratios used.

Table 1 – Structural member details of the 5-storey buildings

<b>Ottawa and Vancouver Buildings</b>		
	Size	Reinforcement
Corner Column 1-5	300X300	8-20M
Ext Column 1-2	300X300	4-25M+4-15M
Ext Column 3-5	300X300	4-25M
Int-1 Column 1-2	400X400	12-25M
Int-1 Column 3-5	400X400	4-25M+4-20M
Int-2 Column 1-2	400X400	4-30M+8-20M
Int-2 Column 3-5	400X400	4-30M
Int-3 Column 1-2	400X400	4-25M+8-20M
Int-3 Column 3-5	400X400	8-20M
Ext Beam Top	300X500	3-20M
Ext Beam Bottom	300X500	2-20M
Int Beam Top	300X500	3-25M
Int Beam Bottom	300X500	2-25M

### 3. Incremental dynamic analysis (IDA)

The present study focuses on developing fragility response of reinforced concrete frame structures in Canada with regular structural layouts, employing incremental dynamic analysis (IDA). A set of 20 earthquake records were selected and IDA was employed to generate fragility curves. IDA was conducted for each seismic record with incrementally varying intensity levels, resulting in IDA curves that provide a relationship between earthquake intensity and a structural deformation quantity. The maximum inter-storey drift ratio,  $\Theta_{max}$ , was used as a damage measure (DM) in the current investigation. The 5% damped spectral acceleration was used as an intensity measure (IM) at effective period  $T_e$ . Each earthquake record was scaled in such a way that the successive run would always be within 10% of the previous IM level. Hunt and fill algorithm was used to limit the number of runs while covering the entire range of structural performance [18]. Accordingly, the dynamic analysis was first conducted under a reduced earthquake intensity to correspond to a relatively low spectral acceleration of 0.005g to ensure elastic response. In the second analysis, the seismic record was amplified such that the increase in spectral increment was 0.05g with a step increment of 0.025g up to failure. The structural failure was defined either by side-sway collapse (structural instability) or when the rate of change in deformations (the slope of the IDA curve) reached 20% of the initial effective elastic slope as also defined in FEMA 350 [19]. Side-sway collapse was defined as the point of dynamic instability when inter-storey drift increased without bound [20]. Fig. 2 illustrates the definition of maximum drift capacity used in the current study. IDA was used to develop fragility response for different performance levels with associated limit states.

### 4. Modelling for Dynamic Analysis

IDA was conducted using software PERFORM-3D [21] for nonlinear dynamic analysis and the evaluation of inelastic performance for structural components. PERFORM-3D is specialized software for damage assessment, and has been used by previous researchers [22, 23, 24, 25, 26]. The frame structures designed earlier were first modelled for dynamic analysis. The frame elements (beam and columns) were modeled to deform in double curvature with two symmetrical segments. Each segment consisted of an elastic beam element and a plastic hinge. Chord rotation was used to define the member end rotation. All the beam and column elements had stiff end zones at the joints that represented the end portions built integrally with the adjoining members. The

stiffness of these end zones were assigned a value equal to 10 times the member stiffness. Fig. 3 shows a schematic diagram for a concrete frame bay with member models incorporated.

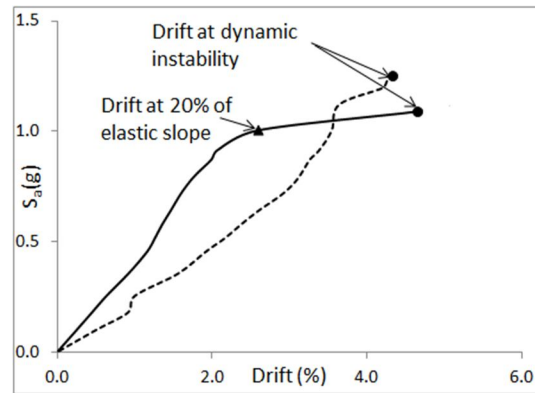


Fig. 2 – Maximum inter-storey drift capacity on IDA Curve

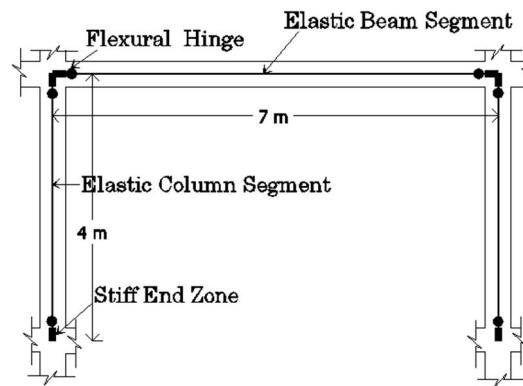


Fig. 3 –Concrete frame elements and analytical member models for PERFORM-3D analysis.

Element rigidities were specified as per the requirements of CSA A23.3-04. Both beam and column rigidities were reduced to account for concrete cracking, and effective inertia,  $I_e$ , were assigned to the members. Hysteretic behavior of potential plastic hinge regions was modelled by assigning the stiffness degrading hysteretic model in PERFORM-3D. The software uses perfectly elasto-plastic hysteretic relationship, modified for stiffness and strength degradation under reversed cyclic loading as illustrated in Fig. 4. The stiffness degradation is introduced through the “energy degradation factor (EDF),” which is the ratio of the area under elasto-plastic and stiffness degrading hysteresis loops. EDF was computed from experimental observations. Tests of reinforced concrete elements conducted by Ozcebec and Saatcioglu [27] were used for this purpose. It was found that well confined flexure-controlled elements showed behaviour that could be modelled with the use of  $EDF = 0.62$  up to the yield point, and  $0.56$  thereafter. The same EDF values were used for both moderately ductile and fully ductile elements.

The envelope curves for the hysteretic models were defined in terms of nominal moment resistances and corresponding chord rotations. This was done according to the ASCE 41-13 [28] guidelines. The yield moment ( $M_Y$ ) and the chord rotation at yield ( $\Theta_Y$ ) were calculated for each element from sectional analysis. The post yield stiffness was defined as strain hardening stiffness with 3% and 4% of the effective elastic stiffness for beam and column elements, respectively up to the ultimate capacity ( $M_U$ ). The ultimate capacity depended on the ductility ratios adopted for moderately ductile and fully ductile structures. The ductility related force modification factor ( $R_d$ ) values, specified in the 2010 NBCC, were used as 2.5 and 4.0 for moderately ductile

and fully ductile buildings. These ductility ratios were also reported to have been observed during previous column tests [29, 30, 31, 32], though some researchers showed that well confined concrete columns could achieve ductility ratios higher than 4.0 irrespective of the level of accompanying axial compression. The ultimate rotational capacity ( $\Theta_U$ ) was defined in the current investigation as 2.5 and 4.0 times the yield rotation ( $\Theta_Y$ ) for moderately and fully ductile elements as the onset of strength decay points. The degradation slope of moment-rotation envelope was computed to be the same as that recommended by ASCE 41-13. The ASCE 41-13 ultimate plastic chord rotation ( $\Theta_U$ ) and the residual moment capacity ( $M_R$ ) depend on the level of axial compression and the confinement steel area ratio. The linear descending branch of the envelop curve continued to the residual moment capacity ( $M_R$ ) as defined in ASCE41-13 as a ratio of the ultimate moment capacity ( $M_U$ ). Fig. 5 shows the details of moment-rotation envelope for members having the same yield capacity, but different levels of ductility.

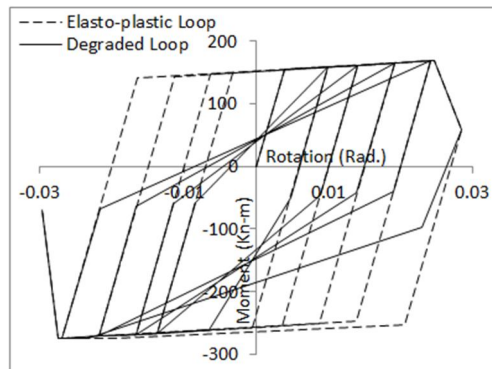


Fig. 4 – Effect of EDF on a Moment vs Total Chord Rotation hysteresis loop area in PERFORM-3D

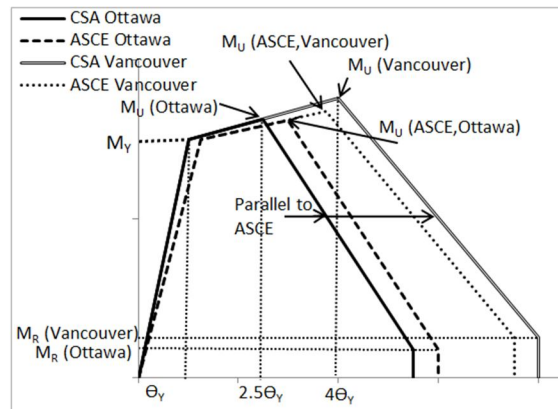


Fig. 5 – Typical moment-rotation envelope curve for same yield capacity member

The members were modelled to behave elastically in shear. This is consistent with CSA A23.3-04, which requires higher shear capacity than that corresponding to flexural capacity to prevent brittle shear failure while promoting ductile flexural response, as preferred performance observed by researchers [33]. Ozcebec and Saatcioglu (1989) [34] experimentally observed that deflections due to shear in flexure-dominant members accounted for 22% of the total deflection, even though local shear deformations within the plastic hinge could be as high as 83% of the hinging region deformation. The contribution of shear to total member deflection was observed to decrease (forming 8% of total deflection in one column test) as inelastic deformations increased in flexure [32]. Linear elastic shear properties of structural elements were also used by previous researches [35,36,37].

## 5. Selection of Earthquake Records

Synthetic earthquake records, developed for Ottawa and Vancouver, with 2% probability of exceedance in 50 years were selected for the development of the fragility curves. These records were compatible with the Uniform Hazard Spectra (UHS) specified in NBCC (2010), and were developed by Atkinson (2009) [38]. The records were modified as suggested by Atkinson (2009) to match the UHS for the period range of interest. The design period ( $T_d$ ) of the buildings considered in the current investigation varied between 0.5 and 2.0 seconds, and this range was used to modify the records. A set of twenty records was selected for buildings in Ottawa, and another set of twenty records was selected for buildings in Vancouver. Each set of records reflected two different magnitudes and two different distances, resulting in four different magnitude-distance combinations. 5 records were selected from each magnitude level and distance category. For Ottawa, M6 earthquakes were selected with epicentral distances of 10-15 km and 20-30 km; and M7 earthquakes were selected with epicentral distances of 15-25 km and 50-100 km. Duration of the records were 5, 7, 17 and 20 seconds, respectively. For Vancouver, M6.5 earthquake was selected with epicentral distances of 10-15 km and 20-30 km; and M7.5 earthquake was selected with epicentral distances of 15-25 km and 50-100 km. The durations of records were 10, 15, 65 and 57 seconds, respectively. Acceleration response spectra were generated for 5% of critical damping and for Soil Type C. Fig. 6 shows the comparison of response spectra for mean seismic records with the UHS of NBCC (2010) for Ottawa and Vancouver.

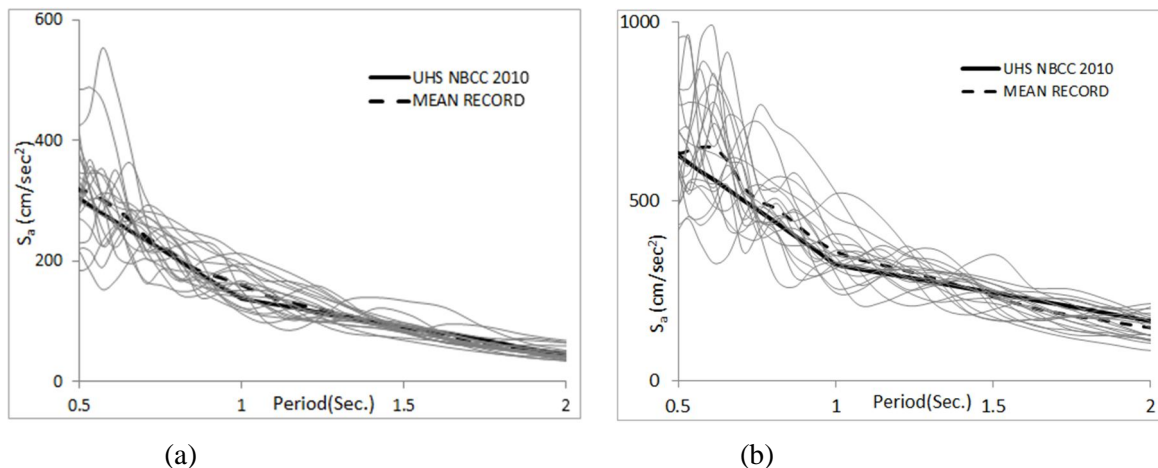


Fig. 6 – Comparison of mean spectral acceleration of seismic records with NBCC (2010) UHS for (a) Ottawa and (b) Vancouver

Fragility analysis required IDA under different intensity of earthquakes. This necessitated the amplification of seismic records. Though it is common to amplify seismic records based on the spectral acceleration at fundamental period [39], researchers used several different approaches to amplify seismic records. Jeong et al. (2012) [40] used effective fundamental period based on pushover analysis. Kircil and Polat (2006) [41] used elastic fundamental period as the reference point. In the present study seismic records were scaled to match the target spectral values obtained by the hunt and fill algorithm discussed earlier to represent different earthquake intensities. This scaling was done using the spectral acceleration value that corresponded to the effective period computed by dynamic analysis using cracked (effective) moment of inertia,  $T_e$ .

For each target spectral acceleration, seismic record was multiplied by a factor equal to  $S_a(\text{Target})/S_{a,T_e}$ , where  $S_a(\text{Target})$  is the target spectral acceleration and  $S_{a,T_e}$  is the spectral acceleration at effective period ( $T_e$ ). The amplification procedure was validated against the spectra of scaled records, where the spectra were computed using software PRISM [42]. In all cases the amplified record was able to generate spectral values that matched  $S_a(\text{Target})$ . This is shown Fig. 7. The scaled records were then used to perform incremental dynamic analysis (IDA).

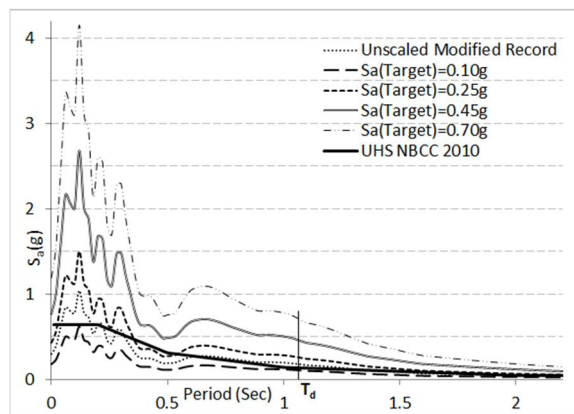


Fig. 7 – Validation of seismic record amplification procedure

## 6. Limit States

The fragility curves were developed for different levels of performance. Commonly accepted performance levels were selected [28, 43, 44]. They consist of; i) Immediate Occupancy (IO), ii) Life Safety (LS), and iii) Collapse Prevention (CP). Inter-storey drift ratio was used as a damage indicator, defining the limit state for each performance level. The recommendations for inter-storey drift limits were adopted from ASCE 41-13, FEMA 356 and ACI 374.2R-13 as 1% and 2% for IO and LS performance levels. The CP performance limit state depended on the onset of strength decay, which in turn depended on the ductility capacity of structural elements. Jeong et al. (2012) [45] used FEMA 356 limit of 4% inter-storey drift, Akkar et al. (2005) [46] used 75% of the median of maximum inter-storey drifts from the records considered, Erberik (2008) [47] used 75% of the mean of maximum inter-storey drifts, Kircil and Polat (2006) used 5% probability of attaining collapse with 95% confidence level, and Ellingwood et al. (2007) [48] used the median of maximum inter-storey drift ratio. In the current investigation CP limit state was defined as the median of the maximum inter-storey drift ratio attained on the IDA curve.

The IO limit represents very limited structural damage, where the force resisting system nearly retains the pre-earthquake strength and stiffness. Since the risk of fatal injury is very low, the building can be reoccupied immediately. Various approaches were performed by researchers to identify IO limit state drift. Jeong et al (2012) used inter-storey drift corresponding to first yield of a structural member, Akkar et al. (2005) used global yield drift ratio, and Kircil and Polat (2006) used maximum inter-storey drift ratio at 5% yield probability of structure with 95% confidence level. Erberik (2008) used softening index (SI) proposed by DiPasquale and Cakmak (1987) [49] to define serviceability limit state, analogous to IO. SI was defined as shown below in Eq. (1):

$$SI = 1 - T_e/T_j \quad (1)$$

where  $T_j$  is effective period at intermediate spectral acceleration.  $SI = 0.20$  was attained at IO limit state when  $T_j = 1.25 T_e$ . This measure of performance was believed to be more reliable than using 1% drift as a criterion since SI provided inter-storey drift ratio for IO performance level corresponding to the seismic records.

## 7. Development of Fragility Relationships

The probability of drift demand (D) at a given Intensity Magnitude,  $S_a(T_e)$ , was calculated according to the method described by Cornell et al. (2002) [50]. The conditional median of drift demand, DM, was expressed as a power-law function,  $DM = a[S_a(T_e)]^b \epsilon$ ; where a and b were regression coefficients and  $\epsilon$  was lognormal random variable [51]. It was assumed that the demand had lognormal probability distribution at a given spectral acceleration with the median lognormal random variable was unity ( $\epsilon = 1$ ). Logarithmic standard deviation of lognormal random variable ( $\sigma_{ln\epsilon}$ ) was equal to the standard deviation of log of demand ( $\sigma_D$ ) [45]. The regression coefficient of power law function was calculated by linear regression in logarithmic space of the ‘cloud’ response using least square method. The standard deviation of log of demand ( $\sigma_D$ ) was assumed constant with

variation of spectral acceleration,  $S_a(T_e)$ . The value of regression coefficient  $a$  and  $b$  and standard deviation of log of demand ( $\sigma_D$ ) were shown in Fig. 8 for both Ottawa and Vancouver structures where analysis were performed with amplified seismic records based on  $S_a(T_e)$ . The dispersion for all the limit states ( $\sigma_{LS}$ ) was considered as 0.3 [40] and the uncertainty in analytical modeling ( $\sigma_M$ ) was taken as 0.2 with 90% confidence that the analytical model findings are within 30% of actual value [48]. The effect of aleatoric and epistemic uncertainty was calculated according to Eq. (2) as proposed by Zareian and Krawinkler (2007) [52]:

$$\sigma_{\text{EQU}} = \sqrt{(\sigma_{\text{LS}}^2 + \sigma_M^2)} \quad (2)$$

Where  $\sigma_{\text{EQU}}$  is the uncertainty component associated with aleatoric and epistemic effect in demand estimation and found to be 0.36 in this study. The total uncertainty in finding the probability of collapse,  $\sigma_{\text{TOT}}$ , was calculated according to Eq. (3).

$$\sigma_{\text{TOT}} = \sqrt{(\sigma_{\text{EQU}}^2 + \sigma_D^2)} \quad (3)$$

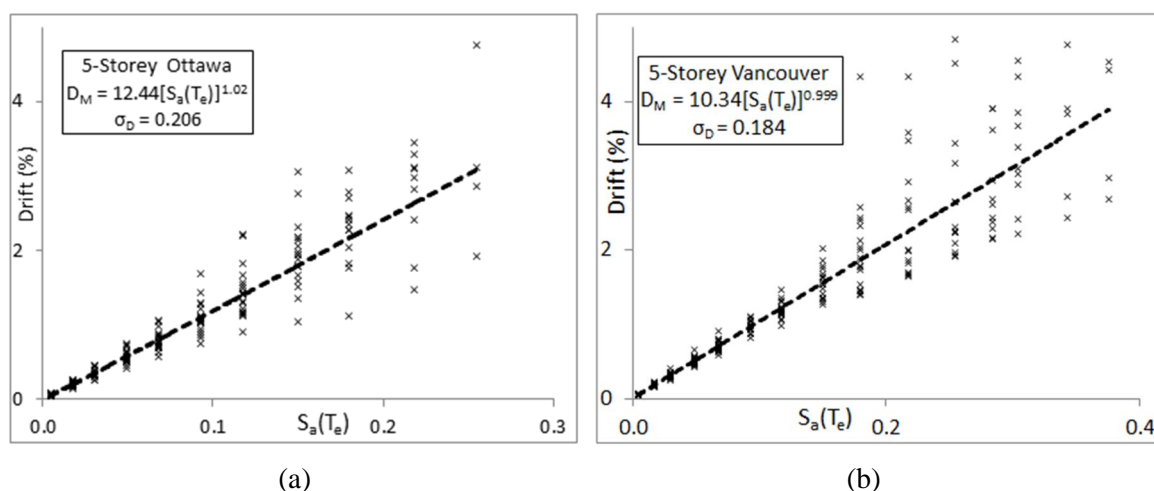


Fig. 8 – Regression analysis of 5-storey structures in (a) Ottawa and (b) Vancouver

## 8. Seismic Performance Evaluation

The 5-storey buildings used in this investigation showed a sequence of hinging that is typical of reinforced concrete frame response under increasing earthquake intensity. The yielding of the beams was observed prior to developing the IO performance level. The beam yielding occurred at lower floors first, followed by the yielding of the first-storey columns. Upon yielding of the columns, inter-storey drift levels increased considerably. At the LS performance level, almost all the first-storey columns had hinged, with the propagation of beam hinging toward the upper floors as buildings approached the CP performance level. The structures reached collapse upon the failure of beams at the 3rd, 4th, 5th and 2nd floor levels, followed by the collapse of the columns at the ground floor level. For the same performance level, more hinging was observed in the building located in Ottawa than the building in Vancouver. Since the onset of strength degradation of moderately ductile structural elements started at lower rotational values than the ductile structural elements, the maximum inter-storey drift at collapse was lower for the building in Ottawa than the building in Vancouver. The CP performance level was reached at 2.94% and 3.91% inter-storey drift ratios for the buildings in Ottawa and Vancouver, respectively.

The fragility curves for the 5-storey buildings selected for Ottawa and Vancouver are shown in Fig. 9. The probabilities of exceedance at different limit states are summarized in Table 2. It was observed that the building in Ottawa had 13% and 27% less probability of exceeding the IO and the CP performance levels in comparison to the building in Vancouver. Hence it can be concluded that the Ottawa building has more margin of safety in

terms of exceeding the performance levels, even though it has a lower drift capacity at the collapse prevention level.

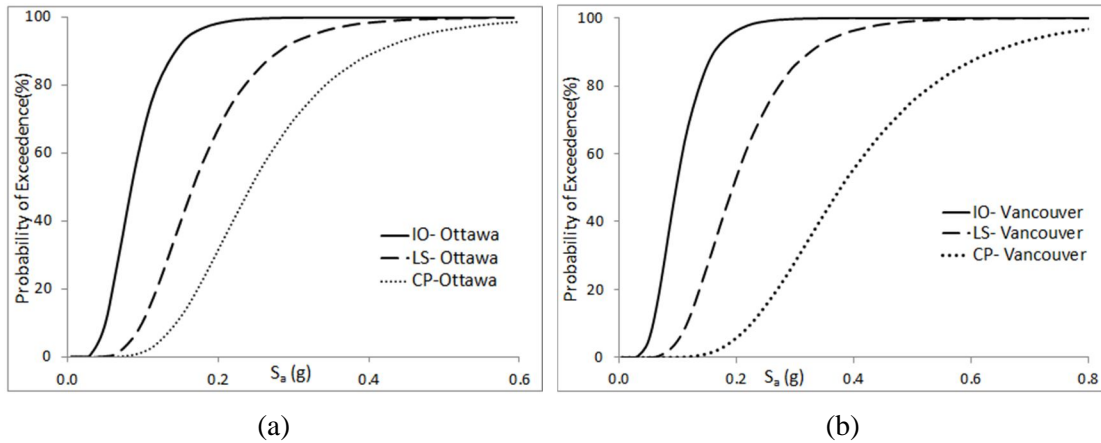


Fig. 9 – Fragility response 5-storey structures in (a) Ottawa and (b) Vancouver

Table 2 – Comparison of limit state probabilities of 5-storey structures

City	$T_d$ , sec	$T_e$ , sec	$S_a(T_d)$ , g	$S_a(T_e)$ , g	Probability of Exceedance at $S_a(T_d)$		
					Performance Levels		
					IO	LS	CP
Ottawa	1.064	2.042	0.134	0.046	87%	30%	7%
Vancouver	1.064	2.042	0.320	0.170	100%	89%	34%

## 9. Conclusion

The fragility curves developed for the 5-storey frame buildings designed for Ottawa and Vancouver indicate that the probability of exceeding the IO performance level at design earthquake intensity was 87% and 100%, respectively. At the same level of intensity, the building in Ottawa developed 30% probability of exceeding the LS performance level, while the building in Vancouver showed 89% probability of exceedance. The probability of exceeding CP level was 7% and 34% for buildings in Ottawa and Vancouver, respectively. It should be noted that these values were obtained for the specific buildings designed with regular plan and elevation layouts based on the seismic detailing requirements of post-1985 practice in Canada, reflecting the current design practice. When the softening of structures under increasing earthquake intensity is considered with elongation of periods (resulting in effective periods  $T_e$ ), the probabilities of exceedance at each performance level became less than the corresponding levels based on the design periods. Table 2 summarizes the performance of buildings at the three selected performance levels.

## 10. References

- [1] GSC (2015). *Geological Survey of Canada*. Earthquake Zones in Canada. Available at <http://www.earthquakescanada.nrcan.gc.ca/zones/index-en.php> (Last accessed 12 May 2016)
- [2] Mitchell D., Paultre P., Tinawi R., Saatcioglu M., Tremblay R., Elwood K., Adams J., DeVall R. (2010). Evolution of seismic design provisions in the national building code of Canada. *Canadian J. of Civil Engng*, 2010, 37(9): 1157-1170
- [3] NBCC (1953). National building code of Canada 1953. *National Research Council of Canada*. Ottawa, Canada.
- [4] NBCC (1965). National building code of Canada 1965. *National Research Council of Canada*. Ottawa, Canada.
- [5] NBCC (1970). National building code of Canada 1970. *National Research Council of Canada*. Ottawa, Canada.
- [6] NBCC (1975). National building code of Canada 1975. *National Research Council of Canada*. Ottawa, Canada.

- [7] NBCC (1980). National building code of Canada 1980. *National Research Council of Canada*. Ottawa, Canada.
- [8] NBCC (1985). National building code of Canada 1985. *National Research Council of Canada*. Ottawa, Canada.
- [9] NBCC (1990). National building code of Canada 1990. *National Research Council of Canada*. Ottawa, Canada.
- [10] NBCC (2005). National building code of Canada 2005. *National Research Council of Canada*. Ottawa, Canada.
- [11] NBCC (2010). National building code of Canada 2010. *National Research Council of Canada*. Ottawa, Canada.
- [12] NBCC (2015). National building code of Canada 2015. *National Research Council of Canada*. Ottawa, Canada.
- [13] CSA (1973). Design of concrete structures. CSA standards update service. *Canadian Standards Association*. CSA A23.3-1973.
- [14] CSA (1984). Design of concrete structures. CSA standards update service. *Canadian Standards Association*. CSA A23.3-1984.
- [15] NRCC (1993). Manual for Screening of Buildings for Seismic Investigation. *National Research Council of Canada*. ISBN 0-660-15381-5. NRCC 36943. Ottawa, Canada.
- [16] CSA (2004). Design of concrete structures. CSA standards update service. *Canadian Standards Association*. CSA A23.3-04.
- [17] CSI (2008). ETABS. Nonlinear Version 9.5.0. *Computers and Structures, Inc.* Berkeley, CA.
- [18] Vamvatsikos D., Cornell C.A. (2004). Applied incremental dynamic analysis. *Earthquake Spectra*. Vol 20, No. 2, Page 523-553, May 2004
- [19] FEMA (2000a). Recommended seismic design criteria for new steel moment-frame buildings. *Federal Emergency Management Agency*. SAC Joint Venture. FEMA 350.
- [20] Goulet C.A., Haselton C.B., Mitrani-Reiser J., Beck J.L., Deierlein G.G., Porter K.A., Stewart J.P. (2007). Evaluation of the seismic performance of a code-conforming reinforced-concrete frame building—from seismic hazard to collapse safety and economic losses. *Earthquake Engineering & Structural Dynamics*. Volume 36, Issue 13, pages 1973–1997.
- [21] CSI (2013). PERFORM-3D. Version 5.0.1. *Computers and Structures, Inc.* Berkeley, CA.
- [22] Reyes J.C., Chopra A.K. (2012). Modal pushover-based scaling of two components of ground motion records for nonlinear RHA of structures. *Earthquake Spectra*. August 2012, Vol. 28, No. 3, pp. 1243-1267
- [23] Ghodsi T., Ruiz J.A.F. (2010). Pacific earthquake engineering research/seismic safety commission tall building design case study 2. *The Structural Design of Tall and Special Buildings*. Volume 19, Issue 1-2, pages 197–256, 2010
- [24] Tuna Z. (2012). Seismic Performance, Modeling, and Failure Assessment of Reinforced Concrete Shear Wall Buildings. *Ph.D. Thesis*. University of California. Los Angeles.
- [25] Liao W. C. (2010). Performance-based plastic design of earthquake resistant reinforced concrete moment frames. *Ph.D. Thesis*. University of Michigan.
- [26] Hopper M. W. (2009). Analytical models for the nonlinear seismic response of reinforced concrete frames. *M.Sc. Thesis*. Pennsylvania State University.
- [27] Ozcebe, G., Saatcioglu, M. (1987). Confinement of concrete columns for seismic loading. *ACI Structural Journal*. Volume 84, Issue 4, Pages 308-315.
- [28] ASCE (2014). Seismic evaluation and retrofit of existing buildings. *American Soc. of Civil Engineers*. ASCE/SEI41-13.
- [29] Park R., Priestley M.J.N., Gill W.D. (1982). Ductility of square-confined concrete columns. *Journal of the Structural Engineering*, ASCE. Vol. 108, No. ST4. April 1982, pp. 929-950.
- [30] Beng Ghee, A., Priestley M.J.N., Park R. (1981). Ductility of reinforced concrete bridge piers under seismic loading. Report 81-3, Department of Civil Engineering, *University of Canterbury*, New Zealand, February 1981.
- [31] Zahn F.A., Park, R., and Priestley M.J.N. (1986). Design of reinforced concrete bridge columns for strength and ductility, Report 86-7, Department of Civil Engineering, *University of Canterbury*, New Zealand, March 1986.
- [32] Saatcioglu M., Ozcebe G. (1989). Response of reinforced concrete columns to simulated seismic loading. *ACI Structural Journal*. Volume 86, Issue 1, pp. 3-12.

- [33] Priestley M., Verma R., Xiao Y. (1994). Seismic Shear Strength of Reinforced Concrete Columns. *Journal of the Structural Engineering*, ASCE. Volume 120, Issue 8, pp. 2310–2329.
- [34] Ozcebe G., Saatcioglu M. (1989). Hysteretic shear model for reinforced concrete members. *Journal of the Structural Engineering*, ASCE. Volume 115, Issue 1, pp. 132-148.
- [35] Borzi B., Pinho R., Crowley H. (2008). Simplified pushover-based vulnerability analysis for large-scale assessment of RC buildings. *Engineering Structures*. Volume 30, Issue 3, pp. 804-820.
- [36] Inel M., Ozmen H.B. (2006). Effects of plastic hinge properties in nonlinear analysis of reinforced concrete buildings. *Engineering Structures*. Volume 28, Issue 11, pp. 1494-1502.
- [37] Liel A.B., Haselton C.B., Deierlein G.G. (2011). Seismic collapse safety of reinforced concrete buildings. II: Comparative assessment of nonductile and ductile moment frames. *J. of the Struc. Engng*, ASCE, 137(4), pp. 492-502.
- [38] Atkinson G.M. (2009). Earthquake time histories compatible with the 2005 National building code of Canada uniform hard spectrum. *Canadian Journal of Civil Engineering*. Volume 36, Number 6, pp 991-1000.
- [39] Vamvatsikos D, Cornell CA (2002): Incremental dynamic analysis. *Earthquake Engineering & Structural Dynamics*, 31 (3), 491-514.
- [40] Jeong S.H., Elnashai A.S. (2007). Probabilistic fragility analysis parameterized by fundamental response quantities. *Engineering Structures*. Volume 29, Issue 6, Pages 11238-1251.
- [41] Kircil M.S., Polat Z. (2006). Fragility analysis of mid-rise R/C frame buildings. *Engineering Structures*. Volume 28, Issue 9, July 2006, Pages 1335-1345.
- [42] PRISM (2011). Version 1.1. *Earthquake Engineering Research Group*. Department of Architectural engineering, INHA University, South Korea.
- [43] FEMA (2000). Prestandard and commentary for the seismic rehabilitation of buildings. *Federal Emergency Management Agency*. FEMA 356.
- [44] ACI (2013). Guide for testing reinforced concrete structural elements under slowly applied simulated seismic loads. *ACI committee 374*. American Concrete Institute. ACI 374.2R-13
- [45] Jeong S.H., Mwafy A.M., Elnashai A.S. (2012). Probabilistic seismic performance assessment of code-compliant multi-story RC buildings. *Engineering Structures*. Volume 34, January 2012, Pages 527-537.
- [46] Akkar S., Susuoglu H., Yakut A. (2005). Displacement-Based Fragility Functions for Low- and Mid-rise Ordinary Concrete Buildings. *Earthquake Spectra*. Volume 21, No. 4. pp. 901-927.
- [47] Erberik M.A. (2008). Fragility-based assessment of typical mid-rise and low-rise RC buildings in Turkey. *Engineering Structures*. Volume 30, Issue 5, pages 1360-1374.
- [48] Ellingwood B.R., Celik O.C., Kinali K. (2007). Fragility assessment of building structural systems in Mid-America. *Earthquake Engineering and Structural Dynamics*. Volume 36, Issue 13, Pages 1935-1952.
- [49] DiPasquale E., Cakmak A.S. (1987). Detection and assessment of seismic structural damage. *Technical Report NCEER-87-0015*. National Center for Earthquake Engineering Research. State University of New York.
- [50] Cornell CA., Jalayer F., Hamburger RO., Foutch D.A. (2002). Probabilistic basis for 2000 SAC Federal Emergency Management Agency steel moment frame guidelines. *Journal of Structural Engineering*. Volume 128, Special Issue: Steel moment frames after Northridge-PartII. Pages: 526-533.
- [51] Ramamoorthy S., Gardoni P., Bracc, J. (2006). Probabilistic Demand Models and Fragility Curves for Reinforced Concrete Frames. *Journal of the Structural Engineering*, ASCE., Volume 132, Issue 10, pages 1563–1572.
- [52] Zareian F., Krawinkler H. (2007). Assessment of probability of collapse and design for collapse safety. *Earthquake Engineering and Structural Dynamics*. Volume 36, Issue 13, Pages 1901-1914.